Extreme South Pacific Phytoplankton Blooms Induced by Tropical Cyclones

Peter Russell[1] and Christopher Horvat[2]

[1]University of Otago
[2]Brown University

November 24, 2022

Abstract

Wind-driven mixing and Ekman pumping from slow-moving tropical cyclones (TCs) can bring nutrients to the euphotic zone, promoting phytoplankton blooms (TC-PBs) observable by satellite remote sensing. We examine an exceptional (z-score = 18-48) TC-PB induced by category-1 Cyclone Oma near the South Pacific island of Vanuatu in February 2019, the most extreme event in the observed satellite record of South Pacific surface Chlorophyll-a (Chl-a). Examining 15 South Pacific TC-PBs since 1997, we identify a "hover" parameter derivable from storm track data correlated with post-TC surface Chl-a (r=0.83). Using a dataset of synthetic storm tracks, we show revisit times for South Pacific TC-PBs are O(250) years, and O(1,500) years for Oma-scale TC-PBs. The episodic, extreme, but consistent nature of such events means they may imprint on sediment records. If so, we show their signature could be used to reconstruct past TC variability.

Extreme South Pacific Phytoplankton Blooms Induced by Tropical Cyclones

Peter Russell[1,2], and Christopher Horvat[3]

[1]Coastal People: Southern Skies - Centre of Research Excellence, University of Otago, Dunedin, NZ.
[2]Department of Physics, University of Otago, Dunedin, NZ
[3]Institute at Brown for Environment and Society, Brown University, Providence, RI, USA.

Key Points:

- Tropical Cyclone Oma induced an extreme ($\sigma > 18$) surface Chlorophyll-a event in 2019 near Vanuatu
- South Pacific, chlorophyll response is correlated to "hover" parameter derivable from storm track data alone
- Oma-type blooms recur on millenial and longer timescales, and may imprint on sedimentary record.

Corresponding author: Christopher Horvat, horvat@brown.edu

Abstract

Wind-driven mixing and Ekman pumping from slow-moving tropical cyclones (TCs) can bring nutrients to the euphotic zone, promoting phytoplankton blooms (TC-PBs) observable by satellite remote sensing. We examine an exceptional (z-score = 18-48) TC-PB induced by category-1 Cyclone Oma near the South Pacific island of Vanuatu in February 2019, the most extreme event in the observed satellite record of South Pacific surface Chlorophyll-a (Chl-a). Examining 15 South Pacific TC-PBs since 1997, we identify a "hover" parameter derivable from storm track data correlated with post-TC surface Chl-a (r=0.83). Using a dataset of synthetic storm tracks, we show revisit times for South Pacific TC-PBs are O(250) years, and O(1,500) years for Oma-scale TC-PBs. The episodic, extreme, but consistent nature of such events means they may imprint on sediment records. If so, we show their signature could be used to reconstruct past TC variability.

Plain Language Summary

We demonstrate that a relatively weak Tropical Cyclone, Oma, produced the most extreme primary production event observed in the South Pacific satellite record of surface Chlorophyll-a. We examined 154 South Pacific tropical cyclones since 1997 - finding just 15 storms had blooms in their wake, although none compared to the response in the wake of Oma. Phytoplankton blooms require specific conditions for formation, namely that they "hover" in place over a long enough period of time, so that wind-driven upwelling of nutrient rich deep water can enter the sunlit surface layers of the ocean and promote photosynthesis. We can characterize the "hovering" of cyclones using a simple parameter derived from location data alone, and so we examine a 10,000 year synthetic dataset of 96,000 South Pacific tropical cyclone tracks to explore the recurrence period of these blooms. We find that Oma-type blooms recur only once in 1500-2000 years. If biological material from these extreme events reaches the sea floor, the rare but consistent nature of such blooms may be visible in the sedimentary record and help constrain past variability in tropical cyclones.

1 Introduction

Strong winds in tropical cyclones (TCs) lead to turbulent mixing, increasing the depth of the mixed layer, (Dickey et al., 1998; Emanuel, 1999). The curl of TC wind stress also drives Ekman pumping that forces surface waters outwards from the TC core and upwells cold, deep, and nutrient-rich water to replace them. The memory of a TC's passing is often seen as anomalous declines in ocean surface temperature (Fisher, 1958; Leipper, 1967), especially for slow-moving TCs (Price, 1981). Over a period of days to weeks, ocean mixing brings the ocean back to equilibrium (Haney et al., 2012).

Mixing and upwelling due to a TC can trigger a unique biological response. Deep nutrient-rich waters can be mixed into the surface layer, triggering primary production and a TC-wake phytoplankton bloom (TC-PB), detected by ocean color satellites as increased surface Chlorophyll a (Chl-a) (I. Lin et al., 2003) after a TC's passing. PBs play an important role in the uptake of atmospheric carbon and benthic-pelagic coupling, exporting particulate organic material to the deep ocean (Graf et al., 1982; Smith et al., 1996). TC-PBs near land can be amplified by terrestrial rainwater and sediment runoff caused by the TC itself (Zheng & Tang, 2007), however here we will focus on areas away from land boundaries.

Whether a TC-PB occurs depends on interactions between the atmosphere, ocean, and biosphere (I.-I. Lin, 2012). The strength and position of cyclone winds determines the depth of vertical mixing and the amount of Ekman upwelling. If upwelling persists, allowing mixing to incorporate deeper waters, a previously-nutrient-limited bloom can occur. The translation speed of a TC therefore determines the balance of these effects at a specific geographic location. If a TC moves too fast, nutrients may not be entrained into the euphotic zone to promote primary production.

Previous work has focused on TC-wake CHL-a responses in the South China Sea and Pacific storm track regions (I.-I. Lin, 2012; Pan et al., 2018; Wang, 2020). There, anomalous TC-PBs typically account for only a small percentage of total surface Chl-a observed in a typical year (I.-I. Lin, 2012), and likely have little impact on carbon cycling, marine food webs, or sedimentation. Because tropical and sub-tropical regions often harbor deep sub-surface chlorophyll maxima at depths of 100 m or more, (Cullen, 2015), some post-TC increases in surface Chl-a may not be the signal of primary production but instead a vertical redistribution of pre-existing biomass from wind-driven vertical mixing (Chai et al., 2021).

Here, we use ocean color satellites and storm track data to present a first study of TC-PBs in the South Pacific, prompted by the observation of an extreme TC-PB from the Category 1 TC Oma. Observed surface Chl-a over two weeks in the wake of TC Oma exceeded climatology by 1020%, and cannot be explained as a vertical redistribution of sub-surface biomass. From 1997-present, we identify 15 South Pacific TC-PBs, finding surface Chl-a response is correlated (Ezekiel's adjusted r=0.83) to a "hover" parameter quantifiable from storm track data alone. We use a synthetic storm track dataset (Bloemendaal et al., 2020) to quantify the statistical properties of TC-PBs in the South Pacific, including the scaling behavior of the hover parameter and the revisit time of large TC-PBs. Because Oma-scale TC-PBs are extreme, rare, and scale with overall TC frequency, we show that observations of increased sedimentation rates induced by Oma-scale South Pacific blooms could allow for a reconstruction of past South Pacific TC frequency.

2 Methods and Data

To observe the surface ocean response to tropical cyclones, we use four separate satellite platforms:

- MODIS (2002-present) is a spectrometer aboard the sun-synchronous AQUA satellite. It passes south-to-north over the equator each afternoon, meaning South Pacific regions are typically imaged near mid-day. The AQUA return period is 2-3 days for the South Pacific and we use MODIS data provided on an approximately equal-area 4.8km grid.
- VIIRS (2012-present) is a spectrometer on board the SUOMI NPP satellite and has a daily revisit time. We use Chl-a data provided on an equal-area 4.8 km grid.
- SeaWIFS (1997-2010) was the sole instrument aboard the OrbView-2 satellite. It had a daily revisit time period we use data provided on an equal-area 9.6km grid.
- HIMAWARI-8 (2015-present) is a geostationary satellite that images the entire South Pacific once per 10 minutes on a nominal 5 km grid. We use daily average composite maps of Chl-a data. The HIMAWARI-8 data provided is not quality controlled, and is susceptible to "speckle" noise around clouds (see e.g., Supporting Figure 1).

Three satellite products (MODIS,VIIRS,SeaWIFS) are obtained on approximately equal-area sinusoidal grids through the NASA Ocean Color Data portal, and we obtain daily composites of near-surface Chl-a using a merged band ratio algorithm and color index scheme for oligotrophic oceans (Hu et al., 2012). This Chl-a retrieval algorithm has been extensively validated against in-situ data and is the standard technique for measuring ocean surface Chlorophyll concentrations. HIMAWARI-8 provides hourly Chl-a data on a fixed, equal-area grid using a similar band ratio and indexing scheme (Murakami, 2016). To compare all satellite data products, each is interpolated to a 0.1° by 0.1° grid by taking the mean of all values closest to a given location in the target grid, excluding those that are cloud-affected. Because clouds are present in all data, we use a 14-day backwards moving average filter to infill missing (cloud-affected) data.

Observed South Pacific TC data (latitude, longitude, translation speed, Saffir-Simpson category, radius to maximum winds) is obtained via the International Best Track Archive for Climate Stewardship (IBTrACS (Knapp et al., 2010)). We use latitude, longitude, category, and radius-to-maximum-wind values provided by the NOAA National Hurricane Center and U.S. Navy Joint Typhoon Warning Centre (JTWC) (*usa_lat*,*usa_lon*,*usa_sshs*, *usa_rmw*). Sections of storm tracks where 3 or more fixes with the distance between fixes < 70 km are investigated. In total 1293 TCs from 1897-2021 had latitude and longitude tracks. Of these 490 were tracked with Saffir-Simpson categories, and 186 were tracked with radius to maximum winds. The average radius to maximum winds of South Pacific TCs is 61.4 km. We include all TCs from the time they are identified as tropical storms ($usa\_sshs \geq 0$). Storm tracks which are not identified with a category ($usa\_sshs = -1$) are excluded, and the first storm where $usa\_sshs > -1$ is in 1956. When necessary, we specify the radius to maximum winds for storms without a measurement as 61.4 km, which yields a total of 267 storms.

Sea surface temperature data is used in concert with Chl-a and storm track data to identify the location of strong upwelling events and pinpoint the location of TC-PBs. Details on the response of the upper ocean to the passing of each TC, the delay between the TC passing and subsequent observed SST anomaly, and surface Chl-a values are provided in the Supporting Information Table S2. For all but one TC, we use Multi-scale Ultra-high Resolution (MUR) SST data (JPL Mur MEaSUREs Project, 2015) to report SST anomalies. The remaining TC (Katrina, 1998) was observed prior to the availability of MUR and MODIS data - we report its Chl-a response using SeaWIFS and SST change from AVHRR Pathfinder SST data (Saha et al., 2018). We also use NOAA Optimum Interpolation 1/4 Degree Daily Temperature Analysis Version 2 SST (Reynolds et al., 2007, OISSTV2) data to confirm and plot SST anomalies (see Fig. 1a).

3 An Extreme Tropical Cyclone-induced Phytoplankton Bloom in the South Pacific

TC Oma was first identified as a Tropical Depression in the Coral Sea region beginning on February 11, 2019. It intensified to Category 1 (Saffir-Simpson scale) on February 15 west of Vanuatu, where it remained until February 18, briefly weakening and then reintensifying, before tracking southwest and transitioning to a Tropical Storm on February 20. The track of TC Oma is shown as a red line in Fig. 1(a), with a blue solid line indicating periods when classified as a Category 1 cyclone and the location of Oma on February 21 shown as a red circle. The upper-ocean response to Oma's presence was confined to an approximately 1.7 million km^2 region west of Vanuatu, a red box in Fig. 1(a).

After TC Oma departed Vanuatu, it left in its wake cold, biomass-rich water. Between February 17 and February 23, sea surface temperatures Fig. 1(a) declined by up to 4.5 degrees, indicating strong Ekman upwelling. Fig. 1(d) shows MODIS-AQUA surface Chl-a detected on February 21, 2019. The cold wake contained high concentrations of surface chlorophyll, in places estimated to exceed 15 mg/m^3. High surface values are not likely to be the result of mixing of a deep Chl-a maximum as may occur in the northwest pacific or in weak observed blooms (Chai et al., 2021). We examine the single bio-ARGO float (ID 6901656) that recorded profiles of chlorophyll, salinity, temperature, and 490nm downwelling irradiance with depth near the WVR (in the period March-May 2015), with average Chl-a, salinity, and temperature values provided in Supporting Figure 2. We find the highest possible Chl-a value that could be recorded by a color satellite due to the mixing of this deep maximum is less than 0.5 mg/m^3 (Supporting Info Text S1). Given that retrieved Chl-a values exceeded 1 mg/m^3 throughout the Oma PB and across

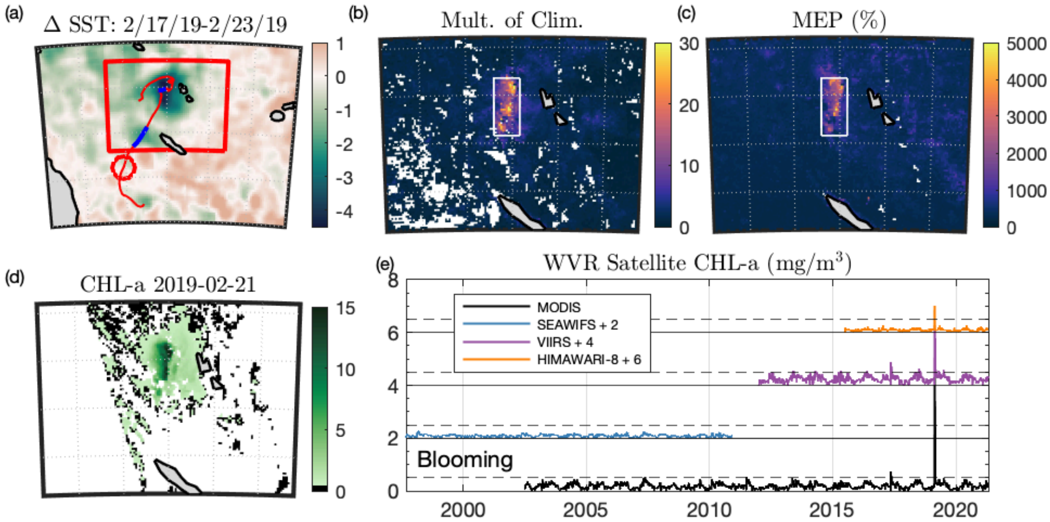

Figure 1. South Pacific response to the passing of Tropical Cyclone Oma. (a) Change in NOAA OISSTV2 sea surface temperature temperature between on Feb 17, 2019 and Feb 23 2019. Red dashed line is trajectory of TC Oma. Blue segments are when Oma was a Category 1 storm. Red box is inset region in (b-d). Red circle is location of Oma on Feb. 21, 2019. (b) Multiple of average Chl-a recorded 2/21/19-3/04/19 from seasonal climatology over same period. White box is "West Vanuatu Region" (WVR). (c) Maximum event percentage (MEP) 2002-present. (d) MODIS-AQUA Chl-a concentration (mg/m^3) on February 21, 2019 in red box of (a). (e) Chl-a measurements in the WVR for ocean color satellites, 1997-present. Plots are offset by +2 for image clarity. Dashed line indicates a "bloom" of 0.5 mg/m^3 for each product.

multiple satellite platforms, we are confident the bloom could not have been due to deep mixing of the sub-surface Chl-a maximum, and we adopt a standard threshold of 0.5 mg/m^3 to identify whether a bloom occurs ((Carstensen et al., 2015)). Here 245,000 km^2 met this threshold within the red box of Fig. 1a. While Oma's cloud cover and the 2-3 day revisit period of the AQUA satellite means there are no MODIS observations of ocean color in this region after Oma arrives and before the 21st, the geostationary HIMAWARI-8 satellite platform confirms the bloom magnitude and extent and its emergence before February 21 (see Fig. 1e, Supporting Figure 1).

The Oma TC-PB was an extreme outlier. Fig. 1(b) shows the ratio of average February 21 - March 4 2019 MODIS-AQUA Chl-a to climatological values for the same annual time period (excluding 2019). Regions locally exceed climatology by up to 4180%. We focus on a 52,000 km^2, region that we term the West Vanuatu Region (WVR) (white contour, Fig. 1c,d), between 14.1° and 17.1°S and 164° and 165.6°E. All MODIS cloud-free values in this box indicated the presence of a bloom on February 21 (Fig. 1d), with an average Chl-a of 4.7 mg/m^3. The two-week climatology was exceeded on average by 1020%. The Oma TC-PB was not only unprecedented for this annual two-week period, but also for any two week period in the observational record. In Fig. 1(c), we plot the maximum two-week event percentage (MEP), computed as:

$$MEP = 100 \times \frac{\text{Maximum average Chl-a over any continuous two week period}}{\text{Average two-week Chl-a}}. \tag{1}$$

MEP quantifies the spatial and temporal localization of blooms. If a region experiences periodic blooming, many large events contribute to the full-period average, and one bloom among many would therefore lead to low MEP values. Average MEP in the South Pacific is 350% - meaning on average the highest two-week Chl-a response from 2002-2021 exceeded 2002-2021 climatology by a factor of 3.5. Within the WVR, MEP values were 1340% on average, and in places exceeded 5000%. Comparable MEP values were not found elsewhere in the South Pacific, rendering the Oma TC-PB the most extreme event in the MODIS record.

A time series of average Chl-a in the WVR is plotted in Fig. 1(e) for the four satellite-derived Chl-a products. All agree on the extreme nature of the OMA TC-PB. Excluding the Oma TC-PB period, average surface Chl-a measurements were 0.18±0.09 mg/m^3 (MODIS), 0.13±0.04 mg/m^3 (SEAWIFS), 0.25±0.12 mg/m^3 (VIIRS), and 0.09±0.03 mg/m^3 (HIMAWARI-8). We compute z-scores for WVR-average Chl-a (C_{WVR})

$$z = \frac{C_{WVR} - \mu_{WVR}}{\sigma_{WVR}}, \tag{2}$$

where σ_{WVR} is the unbiased sample standard deviation of C_{WVR} over the WVR region for the time period preceding the bloom, and μ_{WVR} the mean. Based on WVR-average Chl-a recorded during the peak of the post-Oma bloom, the Oma TC-PB had a z-score of 48 (MODIS), 31 (HIMAWARI-8), or 18 (VIIRS). As extreme TC-PBs recur on periods much longer than the satellite record, z-scores are inappropriate to determinine recurrence times, as they assume normal, well-sampled statistics (for example a 48σ event has a repeat time of once in many times the lifetime of the universe). We quantify return periods using a much longer record of synthetic TC statistics below and merely highlight z-scores to illustrate the extreme nature of the Oma TC-PB over the observed record.

While there are seasonal increases in surface Chl-a in the WVR, blooms are not commonly observed. In the MODIS dataset, the WVR experienced five "bloom" periods (Chl-a>0.5 mg/m^3) from 1997-present, encompassing 38 days. Of those, 16 were part of the Oma TC-PB. The maximum value of MODIS-derived Chl-a in the WVR, not including the Oma TC-PB was 0.75 mg/m^3, making the Oma TC-PB 6.3 times larger than the next highest recorded event on May 12, 2017, which was a TC-PB induced by TC Donna. Donna was the strongest off-season cyclone recorded in the South Pacific, and

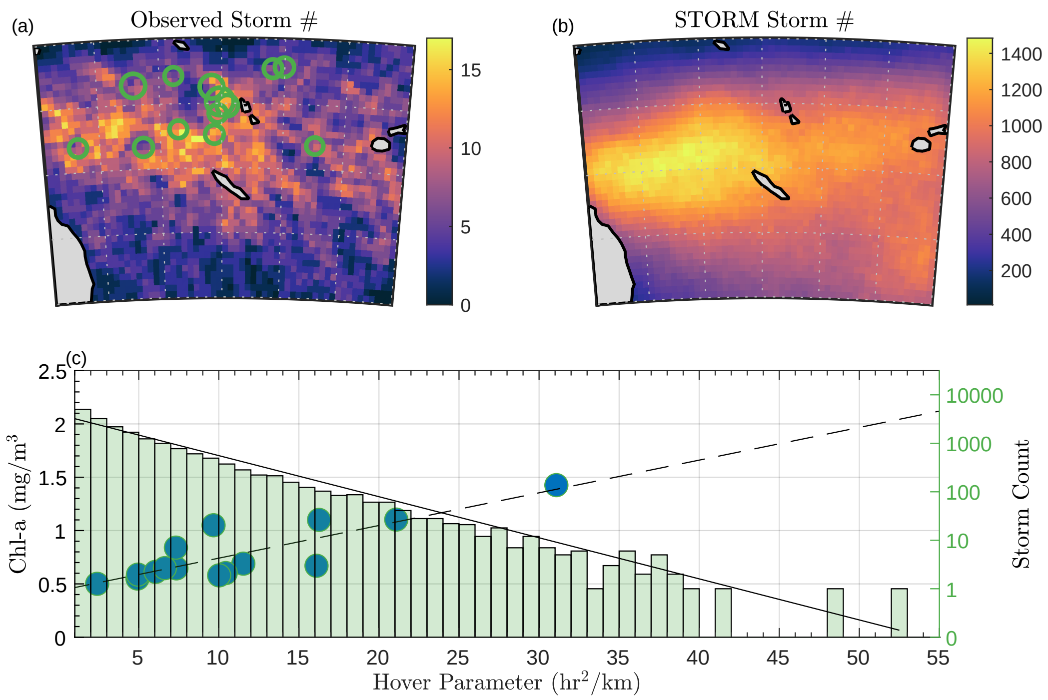

Figure 2. Storm counts and hover parameter scaling in the South Pacific (a) Number of times an IBTrACS TC passes over each South Pacific location within its radius of maximum winds. Green circles are locations of observed TC-PBs. (b) Same as (a), for the STORM dataset. (c) (left axis) Scatter of Chl-a against hover parameter for 15 observed TC-PBs. Dashed line is linear regression fit. (right axis) Number distribution of hover parameter for STORM dataset. Solid line is exponential fit.

produced the largest non-Oma TC-PB, which was recorded by all three active color satellites, centered at 13.7°S, north of the WVR (see Supporting Table S1). No "blooms" other than the Oma TC-PB were observed by SEAWIFS or HIMAWARI-8. The VIIRS dataset records the highest average Chl-a in the WVR, with 140 days as experiencing a bloom, 16 during the Oma TC-PB. Yet if the threshold for a bloom is adjusted to 1 mg/m^3, only the peak of the Donna TC-PB is counted as a "bloom" outside of the Oma TC-PB.

3.1 Tropical cyclone relationship to surface chlorophyll response

We next seek to understand controlling factors on TC-PBs in the tropical South Pacific. To do this we manually identified 15 storms (including Oma) which developed TC-PBs in their wake out of 154 observed South Pacific TCs since 1997. For each South Pacific TC, we examined the local SST anomaly in the wake of each category 1 or higher TC, with large SST anomalies indicating high levels of Ekman upwelling. We then examined locations with strong post-storm SST anomalies for anomalous increases in surface Chl-a.

The locations of the blooms are shown for each storm in Fig. 2a, with details on locations, post-storm SST anomalies and Chl-a response provided in Supporting Information. We also show in Fig. 2(a) show the number of times one of the South Pacific TCs recorded in the International Best Track Archive for Climate Stewardship (IBTrACS) passes over a location within the radius of maximum winds for at least one fix over the storm duration. Locations are on a coarsened to a 0.5x0.5 degree grid, and the count is integrated over all storms. Only 267 of 1293 recorded tracks are included here as they have information about storm strength and pass into the geographic region shown in Fig. 2a. Out of these, on average 12 were recorded over the WVR.

For a TC-PB to occur, wind mixing and Ekman upwelling must combine to allow nutrient-rich water below the euphotic zone to mix into it. This requires cyclone wind-driven mixing, upwelling, and time. Figure 2(c) scatters average TC-PB Chl-a concentrations after the storm (methods) against a "hover parameter", H (units s^2/m), where,

$$H = \int_0^\infty \frac{1}{V}\Theta(V < 3\text{m/s})\, dt \tag{3}$$

where V is the storm translation speed. H describes the period of time during which a storm is translating slowly and is a quadratic function of the storm speed. We use the threshold $V < 3$ m/s as identified in (I.-I. Lin, 2012) used to identify storms that lead to a TC-PB in their wake in the South China Sea and Pacific Storm Track. Surface Chl-a and H for each storm in the South Pacific are listed in Supporting Information Table S1, and are correlated (Ezekiel's adjusted r=0.83). TC Oma is the most extreme, with both the largest value of H and the largest Chl-a response. We determine that a TC-PB occurs when $H > 2$ hr^2/km, below the minimum value (TC Thomas, $H = 2.4$hr^2/km) for the South Pacific TC-PB-producing storms observed here.

Because H is obtained from storm tracks and is correlated to post-storm Chl-a, it can be used to predict the statistics of TC-PBs from storm tracks alone. Observed storm track data is sparse, incomplete, and spans only the most recent century. To derive statistics of South Pacific TC-PBs, we use the Synthetic Tropical cyclOne geneRation Model (STORM) dataset, which provides a 10,000-year record of synthetic storm tracks (Bloemendaal et al., 2020). STORM data resamples statistics based on the International Best Track Archive for Climate Stewardship (IBTrACS) (Knapp et al., 2010) best-track data, with 3-hourly fixes. We compute V using the straight-line distance between successive lat/lon fixes divided by 3 hours. In the South Pacific, there are 93922 individual TC storm tracks, with time series of V, and therefore H. In Fig. 1(b), we repeat Fig. 1(a) using the STORM dataset. An average grid cell in the WVR was passed over by 977 TCs during the 10,000-year STORM period, with 26 having $H > 2$ and 4 having $H > 10$. Note that tracks in the STORM dataset categorizes are all defined tropical cyclones (Saffir-Simpson category >1), whereas the IBTrACS dataset includes weaker tropical storms.

In Fig. 2(c) (right axis, log scale), we plot the number distribution of storms with each H value, $N(H)$. Of all TCs in the South Pacific, 13218 (16.1%) of South Pacific storms met the criteria that $H > 2$, approximately 1 per year, and 1999 (2.3%) have $H > 10$, or 1 per 5 years. These storms with large H we will hereafter define as "Oma-type" TC-PBs.

The long tail of the distribution of H values suggests a consistent scaling behavior. To evaluate the functional distribution of H, we examine maximum likelihood fits for a variety of test distributions (power law, truncated power law, exponential, lognormal, negative binomial, and gamma) using the python *powerlaw* toolbox (Alstott et al., 2014) and following the procedures outlined by (Clauset et al., 2009; Virkar & Clauset, 2014) for testing for scaling behavior. Comparing log-likelihood ratios between all fit pairs we find an exponential fit (solid black line, Fig. 2c),

$$N(H) = 0.195 \exp -0.195(H - 2), \tag{4}$$

compares positively to all others. Python code which ingests the distribution of H values and performs log-likelihood ratio tests is given in the Supporting Information.

An exponential distribution of H underscores the rarity of Oma-type blooms, and can be used to reconstruct total TC count N_{TC} from an observed number of Oma-type blooms N_{oma}. Empirically, a fraction $F = 0.141$ (13218 of 93922) of all STORM tracks have values of $H > 2$. To obtain total TC count, we compute,

$$N_{TC} = \frac{1}{F}\frac{N_{oma}}{\int_2^\infty N(H)dH} \approx 34 \times N_{oma}. \tag{5}$$

3.2 Revisit frequency of TC-PBs

Storms generating TC-PBs occur on sub-decadal timescales across the South Pacific. With TC-PBs comes an anomalous influx of biomass that may play an important role in carbon cycling or marine food webs. Oma-type TC-PBs, which over the course of several weeks may contribute multiple-years of annual primary production, could potentially be seen in sediment - and as their frequency can be related to overall TC frequency, we seek to know where such TC-PBs occur and how often they recur.

To understand likely locations for TC-PBs, in Fig. 3(a) we plot the number of times a distinct TC from the STORM dataset "hovers" over each South Pacific location, and would be expected to lead to a TC-PB (H>2). The revisit frequency is then the expected number of years that would pass between TC-PB events at a location, equal to the STORM dataset length of 10,000 years divided by this TC-PB number. In Fig. 3(b), we plot the latitudinal dependence of the TC-PB number, averaged over longitudes from 150°E to 180°E. Most (71%) of the locations of potential TC-PBs lie in the band between 20°S and 15°S, with local maxima of 31.3 storms at 19.5°S and 33 at 15°S, roughly the location where the Oma TC-PB was observed (green vertical line). For latitudes in this high-storm band, revisit times for TC-PBs are 250-350 years.

Oma-type blooms are significantly rarer, and we repeat Fig. 3(a,b) as Fig. 3(c,d) for those TCs with $H > 10$. While again almost Oma-type events are in the band from 20°S and 10°S, fewer occur than for all TCs capable of producing a TC-PB. The latitudinal average number of Oma-type TC-PB producing storms in the STORM record is everywhere less than 6.1. Locally this may be higher: for example in the region south of Makira (Solomon Is.), 14 Oma-type hover events occur in the STORM dataset. Considering the latitudinal statistics, we estimate a revisit frequency of Oma-type TC-PBs of 1500-2500 years in this high-storm band.

4 Discussion + Conclusions

The phytoplankton bloom in the wake of TC Oma was the most extreme surface Chl-a response recorded by ocean color satellites in the South Pacific since 1997, and covered nearly 250,000 km^2 of Coral Sea west of Vanuatu. Yet Oma was not the only TC-PB recorded in the South Pacific, and we identified 14 others in the study period (1997-present) where anomalous surface Chl-a blooms occurred in the wake of a TC. We identified a correlation between a "hover" parameter, H and the strength of the surface Chl-a response after the TC using satellite derived Chl-a data. Because of the infrequent nature of these events, to understand their statistics we made use of a unique dataset of synthetic storm tracks, which revealed Oma-type blooms revisit a location just once per 1.5-2.5 thousand years.

The observation of TC-PBs is hampered by observational challenges, notably the presence of clouds. In obtaining TC-PB measurements we manually examined all South Pacific TCs using multiple satellite-derived storm track, surface temperature, and surface Chlorophyll-a data (Supporting Tables 1-2). It is possible TC-PBs occurred for some TCs which were not visible from satellite, or that satellite observational uncertainty was responsible for a recorded bloom that may have not occurred. Observations of phyto-

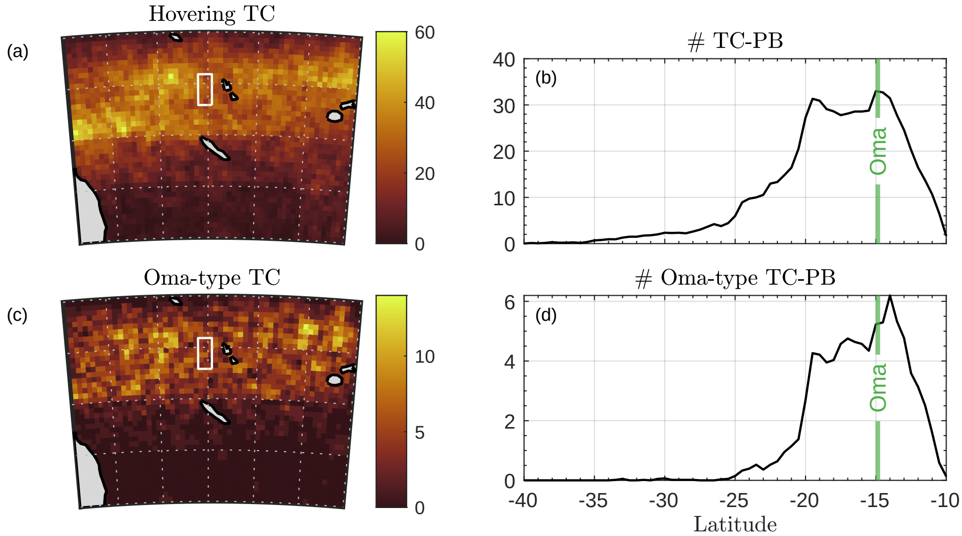

Figure 3. TC-PB revisit frequencies in the South Pacific. (a) Number of times a TC-PB occurs at a given location. White box is the "West Vanuatu Region". (b) Number of TC-PBs as a function of latitude, averaged across longitudes from 150°E to 180°E. Green line is location of Oma bloom. (c,d) Same as (a,b), but for only Oma-type TC-PBs (H>10).

plankton biomass from ocean color satellites are known to exhibit seasonally-varying biases of $\pm$ 20% (Bisson et al., 2021). Because of the highly anomalous (i.e., not systematic) nature of the TC-PBs we observe relative to seasonal Chl-a baselines (increases of 1-2 orders of magnitude from climatology over O(100)$\times 10^3$ km^2), and the multiple satellite platforms that record these events simultaneously, we are confident we are confident these observations are not due to measurement bias. Still, as shown in Fig. 1, the magnitude, location, and extremeness of TC-PBs varies depending on the satellite used. While it is suggested that some TC-PBs are the results of vertical homogenization of existing deep Chlorophyll (Chai et al., 2021), we find that establishing a bloom threshold of 0.5 mg/m^3 rules out this process as generating the anomalous increases in Chl-a observed here.

Primary production is a key driver of the oceanic carbon sink and sedimentation in the deep ocean. Pulses of surface phytoplankton, such as those from PBs, are coupled to the fast-timescale response of benthic communities in the deep ocean (Graf et al., 1982; Billett et al., 1983; Kiørboe et al., 1994; Graf, 1989), including in the tropical Pacific (Smith et al., 1996). Seasonal PBs lead to a flux of phytodetritus to the abyssal oceans (Billett et al., 1983), as they sediment out of the euphotic zone faster than they can be grazed by higher-trophic-level species (Smetacek, 1985). South Pacific TC-PBs are significantly less frequent and more extreme than seasonal blooms, and they occur over areas typically deprived of surface nutrients. It is possible that locally, TC-PBs flux significant and anomalous amounts of carbon and phytodetritus to the abyss.

The infrequency of TC-PBs likely mitigates any long-time-scale impact on regional carbon sequestration in the South Pacific. Yet the fate of TC-PB biomass may be of use in reconstructing past TC variability. Large, infrequent fluxes of phytodetritus to the deep ocean may imprint on the sediment record, recorded in sediment cores as rapid, century-to-millenial-frequency increases in sedimentation rates. Using the exponential scaling of $N(H)$, we found that we may estimate the total number of tropical cyclones using the number of recorded Oma-type blooms as,

$$N_{TC} = 34 \times N(H > 10) \tag{6}$$

Here with N(H>10) = 1999 (in 10,000 years), N_{TC} is estimated as 6.8/yr. Between 1970-2021, 367 TCs were recorded in the South Pacific (Knapp et al., 2010), or 7.2/yr, an accuracy within 6%. The assertion that large TC-PBs may be used to reconstruct past TC counts depends on the ability to resolve TC-PBs in the sediment record, and a more systematic accounting for the fate of biomass from the Oma bloom. With this event occuring in the past decade, we suggest that a shallow sediment core in the WVR could be used to detect sediment from the Oma bloom and therefore the suitability of TC-PBs as a TC proxy. This future direction will require a careful assessment of abyssal South Pacific cores and climate-TC coupling, important areas of current and future work.

Acknowledgments

CH thanks the National Institute of Water and Atmospheric Research in Wellington, NZ for their hospitality during this work. CH was supported in part by Schmidt Futures – a philanthropic initiative that seeks to improve societal outcomes through the development of emerging science and technologies. PR thanks Te Koronga, the Māori research excellence kaupapa (theme) and the Coastal People: Southern Skies Centre of Research Excellence (CoRE) based at the University of Otago for supporting this work. The authors acknowledge the many people of the Pacific who have lost loved ones due to tropical cyclones.

Author Contributions

PR identified present-day TC-PBs and observed the Chl-a/Hover relationship. CH performed the analyses of satellite and storm track data, and prepared the figures. PR and CH wrote the manuscript.

Competing Interests

The authors declare no competing interests.

Open Research

All data used in this manuscript is publicly available. Chl-a data from SEAWIFS, VIIRS, and MODIS-AQUA are available on the NASA Ocean Color Web platform (`https://oceandata.sci.gsfc.nasa.gov/`). Chl-a data from HIMAWARI-8 is available via the JAXA Himawari-8 Monitor (`www.eorc.jaxa.jp/ptree`). IBTRaCS data is available at `ibtracs.unca.edu/`. STORM data is available as Supporting Information to (Bloemendaal et al., 2020). Bio-ARGO data were collected and made freely available by the International Argo Program and the national programs that contribute to it (argo.ucsd.edu, ocean-ops.org). The Argo Program is part of the Global Ocean Observing System. Code used to analyse data and produce figures in this manuscript will be made available as a public github repository with a doi provided by Zenodo upon paper acceptance.

References

Alstott, J., Bullmore, E., & Plenz, D. (2014, jan). powerlaw: a Python package for analysis of heavy-tailed distributions. *PloS one*, *9*(1), e85777. Retrieved from `https://dx.plos.org/10.1371/journal.pone.0085777` doi: 10.1371/journal.pone.0085777

Billett, D. S. M., Lampitt, R. S., Rice, A. L., & Mantoura, R. F. C. (1983, apr). Seasonal sedimentation of phytoplankton to the deep-sea benthos. *Nature*, *302*(5908), 520–522. Retrieved from `http://www.nature.com/articles/302520a0` doi: 10.1038/302520a0

Bisson, K. M., Boss, E., Werdell, P. J., Ibrahim, A., & Behrenfeld, M. J. (2021, jan). Particulate Backscattering in the Global Ocean: A Comparison of Independent Assessments. *Geophysical Research Letters*, *48*(2). Retrieved from `https://onlinelibrary.wiley.com/doi/10.1029/2020GL090909` doi: 10.1029/2020GL090909

Bloemendaal, N., Haigh, I. D., de Moel, H., Muis, S., Haarsma, R. J., & Aerts, J. C. (2020). Generation of a global synthetic tropical cyclone hazard dataset using STORM. *Scientific Data*, *7*(1), 1–12. Retrieved from `http://dx.doi.org/10.1038/s41597-020-0381-2` doi: 10.1038/s41597-020-0381-2

Carstensen, J., Klais, R., & Cloern, J. E. (2015). Phytoplankton blooms in estuarine and coastal waters: Seasonal patterns and key species. *Estuarine, Coastal and*

Shelf Science, *162*, 98–109.
Chai, F., Wang, Y., Xing, X., Yan, Y., Xue, H., Wells, M., & Boss, E. (2021, feb). A limited effect of sub-tropical typhoons on phytoplankton dynamics. *Biogeosciences*, *18*(3), 849–859. Retrieved from `https://bg.copernicus.org/articles/18/849/2021/` doi: 10.5194/bg-18-849-2021
Clauset, A., Shalizi, C. R., Newman, M. E. J., Rohilla Shalizi, C., & J Newman, M. E. (2009). Power-Law Distributions in Empirical Data. *SIAM Review*, *51*(4), 661–703. Retrieved from `http://epubs.siam.org/doi/10.1137/070710111` doi: 10.1137/070710111
Cullen, J. J. (2015). Subsurface chlorophyll maximum layers: Enduring enigma or mystery solved? *Annual Review of Marine Science*, *7*, 207–239. doi: 10.1146/annurev-marine-010213-135111
Dickey, T., Frye, D., McNeil, J., Manov, D., Nelson, N., Sigurdson, D., ... Johnson, R. (1998). Upper-ocean temperature response to Hurricane Felix as measured by the Bermuda Testbed Mooring. *Monthly Weather Review*, *126*(5), 1195–1201.
Emanuel, K. A. (1999). Thermodynamic control of hurricane intensity. *Nature*, *401*(6754), 665.
Fisher, E. L. (1958). Hurricanes and the sea-surface temperature field. *Journal of meteorology*, *15*(3), 328–333.
Graf, G. (1989). Benthic-pelagic coupling in a deep-sea benthic community. *Nature*, *341*(6241), 437–439. doi: 10.1038/341437a0
Graf, G., Bengtsson, W., Diesner, U., Schulz, R., & Theede, H. (1982, apr). Benthic response to sedimentation of a spring phytoplankton bloom: Process and budget. *Marine Biology*, *67*(2), 201–208. Retrieved from `http://link.springer.com/10.1007/BF00401286` doi: 10.1007/BF00401286
Haney, S., Bachman, S., Cooper, B., Kupper, S., McCaffrey, K., Van Roekel, L., ... Ferrari, R. (2012, nov). Hurricane wake restratification rates of one-, two- and three-dimensional processes. *Journal of Marine Research*, *70*(6), 824–850. doi: 10.1357/002224012806770937
Hu, C., Lee, Z., & Franz, B. (2012). Chlorophyll a algorithms for oligotrophic oceans: A novel approach based on three-band reflectance difference. *Journal of Geophysical Research: Oceans*, *117*(1), 1–25. doi: 10.1029/2011JC007395
JPL Mur MEaSUREs Project. (2015). GHRSST Level 4 MUR Global Foundation Sea Surface Temperature Analysis (v4.1). *PO. DAAC.*.
Kiørboe, T., Lundsgaard, C., Olesen, M., & Hansen, J. L. S. (1994, mar). Aggregation and sedimentation processes during a spring phytoplankton bloom: A field experiment to test coagulation theory. *Journal of Marine Research*, *52*(2), 297–323. Retrieved from `http://www.ingentaselect.com/rpsv/cgi-bin/cgi?ini=xref&body=linker&reqdoi=10.1357/0022240943077145` doi: 10.1357/0022240943077145
Knapp, K. R., Kruk, M. C., Levinson, D. H., Diamond, H. J., & Neumann, C. J. (2010, mar). The International Best Track Archive for Climate Stewardship (IBTrACS). *Bulletin of the American Meteorological Society*, *91*(3), 363–376. Retrieved from `https://journals.ametsoc.org/doi/10.1175/2009BAMS2755.1` doi: 10.1175/2009BAMS2755.1
Leipper, D. F. (1967). Observed ocean conditions and Hurricane Hilda, 1964. *Journal of the Atmospheric Sciences*, *24*(2), 182–186.
Lin, I., Liu, W. T., Wu, C.-C., Wong, G. T. F., Hu, C., Chen, Z., ... Liu, K.-K. (2003). New evidence for enhanced ocean primary production triggered by tropical cyclone. *Geophysical Research Letters*, *30*(13).
Lin, I.-I. (2012). Typhoon-induced phytoplankton blooms and primary productivity increase in the western North Pacific subtropical ocean. *Journal of Geophysical Research: Oceans*, *117*(C3).
Murakami, H. (2016, may). Ocean color estimation by Himawari-8/AHI. In

R. J. Frouin, S. C. Shenoi, & K. H. Rao (Eds.), *Remote sensing of the oceans and inland waters: Techniques, applications, and challenges* (p. 987810). Retrieved from http://proceedings.spiedigitallibrary.org/proceeding.aspx?doi=10.1117/12.2225422 doi: 10.1117/12.2225422

Pan, J., Huang, L., Devlin, A. T., & Lin, H. (2018). Quantification of Typhoon-Induced Phytoplankton Blooms Using Satellite Multi-Sensor Data. *Remote Sensing*, *10*(2), 318.

Price, J. F. (1981). Upper ocean response to a hurricane. *Journal of Physical Oceanography*, *11*(2), 153–175.

Reynolds, R. W., Smith, T. M., Liu, C., Chelton, D. B., Casey, K. S., & Schlax, M. G. (2007, nov). Daily High-Resolution-Blended Analyses for Sea Surface Temperature. *Journal of Climate*, *20*(22), 5473–5496. Retrieved from http://journals.ametsoc.org/doi/10.1175/2007JCLI1824.1 doi: 10.1175/2007JCLI1824.1

Saha, K., Zhao, X., Zhang, H., Casey, K., Zhang, D., Baker-Yeboah, S., … Relph, J. (2018). AVHRR Pathfinder version 5.3 level 3 collated (L3C) global 4km sea surface temperature for 1981-Present. *NOAA National Centers for Environmental Information: Asheville, NC, USA*.

Smetacek, V. S. (1985). Role of sinking in diatom life-history cycles: ecological, evolutionary and geological significance. *Marine biology*, *84*(3), 239–251.

Smith, C. R., Hoover, D. J., Doan, S. E., Pope, R. H., Demaster, D. J., Dobbs, F. C., & Altabet, M. A. (1996, jan). Phytodetritus at the abyssal seafloor across 10° of latitude in the central equatorial Pacific. *Deep Sea Research Part II: Topical Studies in Oceanography*, *43*(4-6), 1309–1338. Retrieved from https://linkinghub.elsevier.com/retrieve/pii/096706459600015X doi: 10.1016/0967-0645(96)00015-X

Virkar, Y., & Clauset, A. (2014, mar). Power-law distributions in binned empirical data. *The Annals of Applied Statistics*, *8*(1), 89–119. Retrieved from http://projecteuclid.org/euclid.aoas/1396966280 doi: 10.1214/13-AOAS710

Wang, Y. (2020, oct). Composite of Typhoon-Induced Sea Surface Temperature and Chlorophyll-a Responses in the South China Sea. *Journal of Geophysical Research: Oceans*, *125*(10), e2020JC016243. Retrieved from https://onlinelibrary.wiley.com/doi/10.1029/2020JC016243 doi: 10.1029/2020JC016243

Zheng, G. M., & Tang, D. (2007). Offshore and nearshore chlorophyll increases induced by typhoon winds and subsequent terrestrial rainwater runoff. *Marine Ecology Progress Series*, *333*, 61–74.

Supporting Information for Extreme South Pacific Phytoplankton Blooms Induced by Tropical Cyclones

Peter Russell[1,2] and Christopher Horvat[3]

[1]Coastal People: Southern Skies - Centre of Research Excellence, University of Otago, Dunedin, NZ.

[2]Department of Physics, University of Otago, Dunedin, NZ

[3]Institute at Brown for Environment and Society, Brown University, Providence, RI, USA.

1. Highest Potential Chl-a measurement

To understand whether the Chl-a recorded in the Oma bloom could come from vertical mixing of this deep Chl-a maximum, we compute the average Chl-a value, $\overline{C}(D)$ for a profile $C(z)$ perfectly mixed by a storm to a depth D,

$$\overline{C}(D) = \frac{\int_0^D C(z)\,dz}{D}. \qquad (1)$$

For the Bio-ARGO data obtained in the WVR (Fig. S2) the maximum value of Chl-a is $\overline{C}_{max} = 0.13$ mg/m^3 at $D = -125$m. Color satellites measurements sense Chl-a approximately over the first optical depth, $Z_{90} = 1/\kappa_{490}$, where κ_{490} is the diffuse attenuation coefficient of light at 490nm. We compute κ_{490} by fitting the average downwelling 490nm curve to an exponential function, obtaining $Z_{90} = 37$m for this region of the South Pacific. Assuming that vertical mixing homogenizes the maximum amount of deep Chl-a per meter, and that all of this deep Chl-a is mixed into observable depths, we obtain the highest mixing-sourced Chl-a C_{mix} as,

$$C_{mix} = \overline{C}_{max} \frac{D}{Z_{49}} \approx 0.47 \text{ mg/m}^3. \tag{2}$$

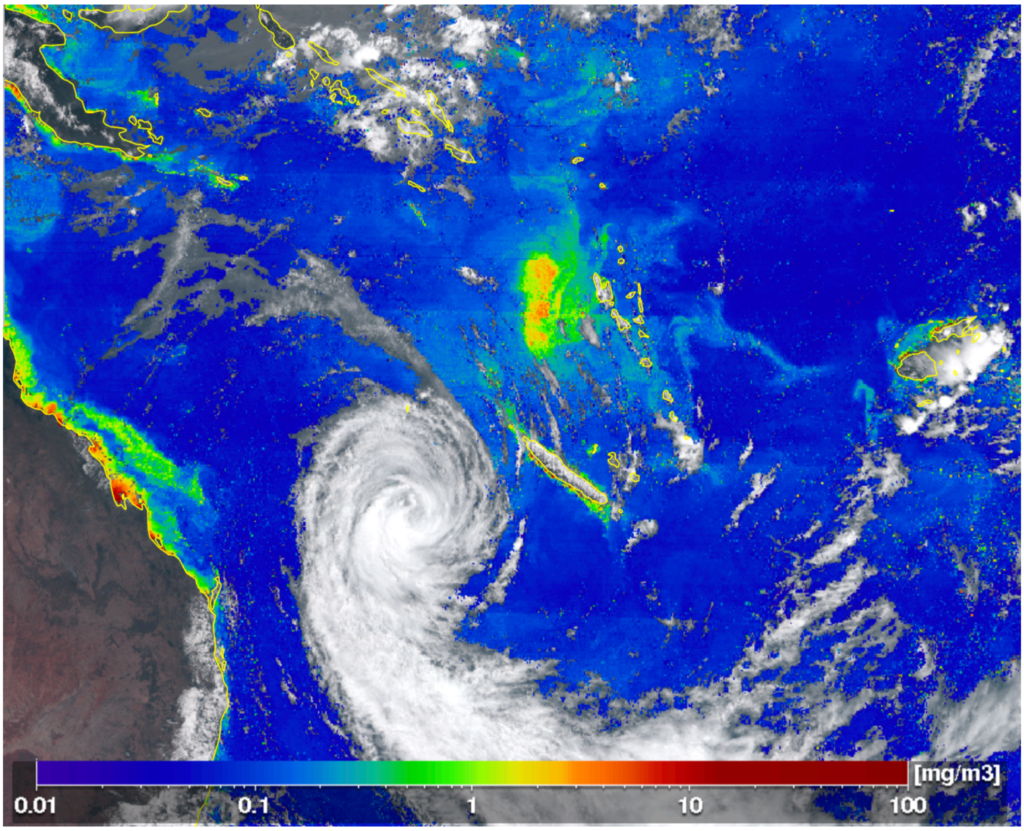

Figure S1. Massive phytoplankton bloom induced by Tropical Cyclone Oma, 21 February 2019, UTC 0.00-0.59. Visible is the TC-PB West of Vanuatu and Cyclone Oma, West of New Caledonia. The Australian East Coast (2000km) provides scale. Chlorophyll model product image (produced from Himawari-8) supplied by the P-Tree System, Japan Aerospace Exploration Agency (JAXA).

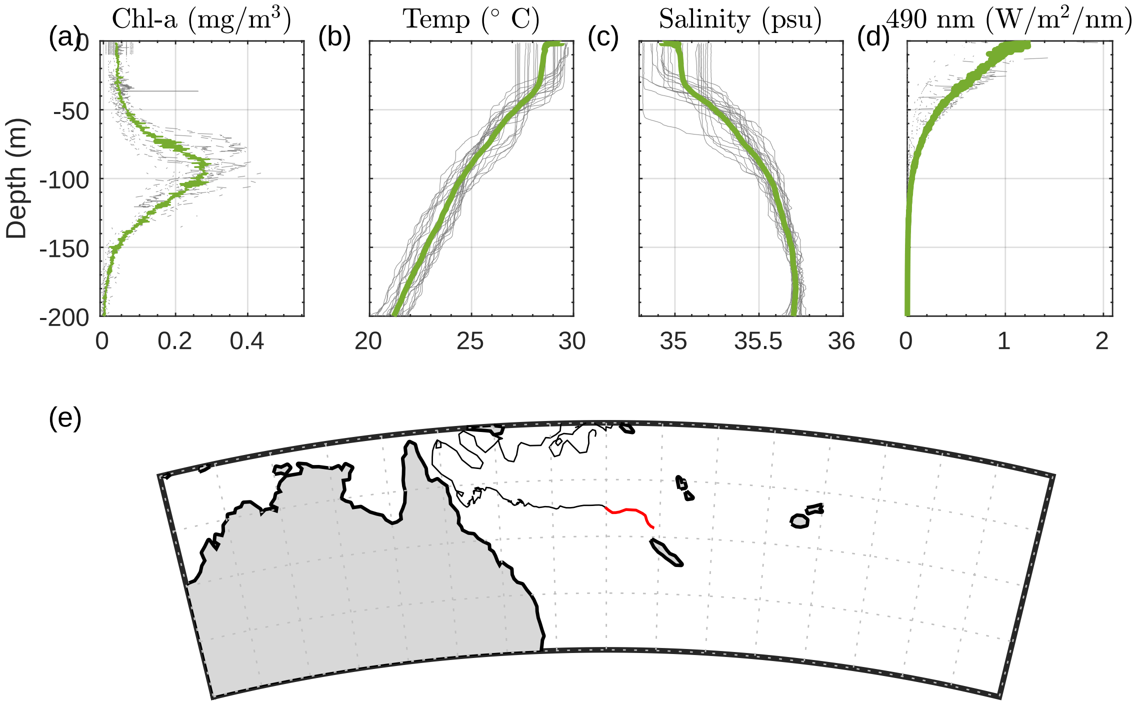

Figure S2. Bio-ARGO float data in the South Pacific. (a) Adjusted Chl-a (mg/m^3) measurements as a function of depth for the first 25 dives (red plot in (e)). Average shown in green. (b,c,d) Same as (a), for temperature, salinity, and 490 nm downwelling irradiance. (e) Location of bio-ARGO float 6901656 over time. Red is the samples used to make (a-d).

Table S1. TC-PB Hover and Chl-a data. Storm name with centre position (lon,lat) of TC-PB, JTWC fix numbers included in hover calculation, hover (H) in hrs^2/km, mean Chl-a $\geq$ 0.5mg/m^3, number of Chl-a 4km grids in mean, date of Chl-a observation with (number of days after significant ΔSST).

Storm	Lon	Lat	Fixes	H (hrs^2/km)	Chl-a ($\geq$ 0.5mg/m^3)	Count	Date (days after ΔSST)
Niran	147.64	-14.37	11-20	16.26	1.10	364	9-Mar-21 (3)
Harold	165.45	-15.18	15-21	7.32	0.84	40	9-Apr-20 (4)
Oma	164.85	-14.86	5-28	31.08	1.43	2820	21-Feb-19 (3)
Hola	164.4	-17.41	14-20	7.35	0.65	7	12-Mar-18 (4)
Donna	164.18	-13.72	14-19	9.67	1.05	894	11-May-17 (5)
Winston	172.63	-18.16	47-53	4.92	0.55	28	28-Feb-16 (6)
Pam	169.96	-12.14	5-14	11.53	0.69	208	17-Mar-15 (3)
Sandra	161.47	-16.98	18-25	4.95	0.59	215	15-Mar-13 (3)
Uliu	157.94	-13.50	18-34	21.08	1.10	102	23-Mar-10 (6)
Thomas	-178.46	-14.68	15-19	2.40	0.50	1	18-Mar-10 (4)
Wati	153.21	-18.10	15-19	6.05	0.61	4	27-Mar-06 (3)
Kerry	158.57	-18.30	18-28	16.10	0.67	54	14-Jan-05 (4)
Beni	161.16	-12.84	4-14	10.02	0.58	66	31-Jan-03 (4)
Zoe	169.06	-12.28	13-19	6.63	0.65	59	3-Jan-03 (4)
Katrina	164.67	-15.78	28-36	10.43	0.60	9	15-Jan-98 (7)

Table S1. Dataset details

Storm	JTWC ID	Chl-a dataset	Grid (E E S S)	Date	ΔSST dataset	Grid (E E S S)	Date
Niran	bsh232021	MODIS	146.48 149.98 -12.98 -15.98	9-Mar-21	MUR	146 150 -13 -16	6-Mar-21
Harold	bsh252020	MODIS	163.98 165.69 -13.98 -16.98	9-Apr-20	MUR	164.0 166.5 -14.0 -17.0	5-Apr-20
Oma	bsh152019	MODIS	161.98 166.48 -12.98 -17.98	21-Feb-19	MUR	160 168 -11 -20	18-Feb-19
Hola	bsh122018	MODIS	162 166 -16 -19	12-Mar-18	MUR	164 168 -15 -20	8-Mar-18
Donna	bsh182017	MODIS	161.98 166.48 -11.98 -16.98	11-May-17	MUR	162.0 166.5 -12.0 -16.0	6-May-17
Winston	bsh112016	MODIS	169.98 173.98 -15.98 -19.98	28-Feb-16	MUR	170 176 -16 -20	22-Feb-16
Pam	bsh172015	MODIS	167.98 173.98 -7.98 -14.98	17-Mar-15	MUR	168 174 -8 -17	14-Mar-15
Sandra	bsh192013	MODIS	157.98 163.98 -13.98 -17.98	15-Mar-13	MUR	158 164 -12 -19	12-Mar-13
Uliu	bsh202010	MODIS	153.98 163.98 -11.98 -16.98	23-Mar-10	MUR	154 164 -9 -17	17-Mar-10
Thomas	bsh192010	MODIS	-179.5 -177 -14 -15.9	18-Mar-10	MUR	-180 -176 -10 -18	15-Mar-10
Wati	bsh182006	MODIS	149.98 157.98 -14.98 -19.98	27-Mar-06	MUR	150 160 -15 -20	24-Mar-06
Kerry	bsh082005	MODIS	155.98 163.982 -14.98 -19.98	14-Jan-05	MUR	156 164 -15 -22	10-Jan-05
Beni	bsh122003	MODIS	157.98163.98 -11.98-13.98	31-Jan-03	MUR	156 164 -9 -16	27-Jan-03
Zoe	bsh062003	MODIS	165.98 171.98 -8.98 -14.98	2-Jan-03	MUR	166 172 -9 -15	30-Dec-02
Katrina	bsh121998	SEAWIFS	161.96 165.96 -14.96 -17.96	15-Jan-98	AVHRR	163.0 166.0 -14.5 -17.0	14-Jan-98